DAMAGE MEASUREMENTS ON THE NWTC DIRECT-DRIVE, VARIABLE-SPEED TEST BED[*†]

Herbert J. Sutherland
Wind Energy Department
Sandia National Laboratory
Albuquerque, NM 87185

Palmer W. Carlin
National Wind Technology Center
National Renewable Energy Laboratory
Golden, Colorado 80401

ABSTRACT

The NWTC (National Wind Technology Center) Variable-Speed Test Bed turbine is a three-bladed, 10-meter, downwind machine that can be run in either fixed-speed or variable-speed mode. In the variable-speed mode, the generator torque is regulated, using a discrete-stepped load bank to maximize the turbine's power coefficient. At rated power, a second control loop that uses blade pitch to maintain rotor speed becomes active. The load bank controller continues essentially as before, i.e., using the load bank to maintain either generator torque or (optionally) generator power. In this paper, we will use this turbine to study the effect of variable-speed operation on blade damage. Using time-series data obtained from blade flap and edge strain gauges, the load spectrum for the turbine is developed using rainflow counting techniques. Miner's rule is then used to determine the damage rates for variable-speed and fixed-speed operation. The results illustrate that the variable speed controller algorithm used with this turbine introduces relatively large load cycles into the blade that significantly reduce its service lifetime, while power production is only marginally increased.

[*]This work is supported by the U.S. Department of Energy under Contract DE-AC04-94AL85000 and DE-AC36-83CH10093. Sandia is a multiprogram laboratory operated by Sandia Corporation, a Lockheed Martin company, for the U.S. Department of Energy.

INTRODUCTION

Variable-speed generator architectures in wind turbines offer the promise of increased energy production and reduced loads through torque control. Most studies have centered on the power production aspects of variable-speed operation[1,2] and only now are its effects on loads being considered.[3-5] In this paper, we use the NWTC Variable-Speed Test Bed turbine[6] to study the effect of variable speed on blade damage. Using time-series data obtained from blade flap and edge strain gauges, the load spectrum for the turbine is developed using rainflow counting techniques. Equivalent data sets, with similar inflow conditions, are taken with the turbine operated in fixed-speed mode. Miner's rule[7] is then used to determine the damage rate for each case. The damage rate for variable-speed operation is compared to that produced in fixed-speed operation.

THE NWTC VARIABLE-SPEED TEST BED TURBINE

The Variable-Speed Test Bed wind turbine[6] is one of two 25-kilowatt (kW) Grumman Windstream 33 turbines at the NWTC. These turbines are three-bladed downwind machines with pitchable blades in a rigid hub. The blade pitch is driven by a variable-speed reversible servo actuator motor either toward stall or toward feather. The original factory-supplied aluminum rotor was 10 meters (33 feet) in diameter.

The Test Bed turbine is equipped with a set of composite blades and a direct-coupled, permanent magnet, 20-kW generator. The original Grumman-supplied blades were replaced with SERI S809 blades.[8]

These blades, which are members of the Solar Energy Research Institute (SERI) airfoil family, are constant chord and not twisted. The rotor diameter remains at 10m (33 feet). Initial computer simulations indicated that this blade set has its best power coefficient at a tip-speed ratio of about 7 with the blade pitch set to 3 degrees. At the rated wind speed, this tip speed ratio translates to a rotor speed of about 100 RPM. This combination of rotor and generator yields a rather low rated power of 5 kW.

The turbine can be run in either fixed-speed or variable-speed mode. In the variable-speed mode, the blade pitch is maintained at 3 degrees of pitch and the generator torque is regulated, using a load bank, to maximize the turbine's power coefficient (aerodynamic efficiency). At rated power a second control loop that uses blade pitch to limit rotor speed becomes active. The load bank controller continues essentially as before, i.e., using the load bank to maintain either generator torque or (optionally) generator power.

Generator

The turbine is fitted with a permanent-magnet, direct-drive prototype generator developed by the University of Colorado Electrical and Computer Engineering Department.[9] The generator is a three-phase, 20-kW generator with a short-term overload capacity of 30 kW. The generator voltage and frequency are directly proportional to generator speed. In the speed range from 0 to 120 revolutions per minute (RPM) the electric frequency varies continuously from zero to 12 hertz. At the same time the line-to-line voltage varies from 0 to 600 volts RMS. The normal operating range has been defined to be from 60 to 120 RPM, which implies 6 to 12 Hz and 300 to 600 V.

In the final configuration the generator system will incorporate custom power electronics to transform the generator's variable output to direct current and then back to utility-grade alternating current. In the present configuration, the power produced by the turbine is not fed into the grid, rather an adjustable load bank with switched contactors is used to load the turbine. The three-phase load bank is formed from eight separate sets of delta-connected resistors, each with its own contactor to connect it to the generator bus. The resistance values of each bank were chosen so that at constant generator voltage, the next larger bank would sink double the current (and power) of the previous bank. Thus, the load bank is capable of 256 different loads that are balanced, three-phase and equally spaced in power. Mechanical relays are used to switch these loads in and out of the generator circuit.

Control System

The turbine is controlled using a personal computer programmed in the C language. An onboard C compiler allows immediate program modifications.

The turbine can be operated in a constant-speed mode or in one of several variable-speed modes. All of the variable-speed algorithms examined to date contain two primary regions of interest. The first is called Region 2 and the second Region 3. In the former, the wind machine is in operation above the cut-in speed, but below its maximum or rated power. In this region maximum energy capture is the desired behavior. In Region 3, the wind machine is in operation at or slightly above its maximum or rated power. In this region, maintaining rated power with due regard for safety, fatigue life, and retention of control is the primary objective. Region 1 of the control algorithm is standby operation below the cut-in wind speed.

In Region 2, the turbine is controlled exclusively by using the load bank (output power). The control system updates the load-bank setting at half-second intervals to one of the 256 discrete loads contained in the bank. In each update cycle, the current rotor speed is determined first. Then, this speed is used with a look-up table to select the appropriate load-bank setting for maximum power production, and finally, the load bank is switched. Qualitatively, note that if the wind is providing more than the requested power, the rotor will accelerate and the next load bank update will request more power. Similarly, on a declining wind the load bank will progressively decrease the requested power. Operation is quite stable. In this region, the blade pitch is fixed at 3 degrees.

In Region 3, two control loops are active. The first is the power control loop used in Region 2 and the second controls blade pitch. The blade-pitch control loop endeavors to limit the rotor speed to 105 RPM. The load control loop has two options. In the first, the load control endeavors to maintain a constant torque corresponding to rated power and in the second, it endeavors to maintain constant rated power. Thus, in Region 3, the controller endeavors to limit the turbine's output torque (or optionally power) and speed to predetermined set points. Fluctuations in speed and the output power are noted in Region 3, albeit with greatly restricted ranges over those observed in Region 2. The transition between Regions 2 and 3 occurs at an inflow speed of approximately 7 m/s (16 mph).

Figure 1 illustrates the typical behavior of the turbine under this control algorithm. This figure reports 100 seconds of data that have been extracted from a 10-minute (600 second) record for illustration purposes. The data start at a record time of 50 seconds and end at 150 seconds. The transition between

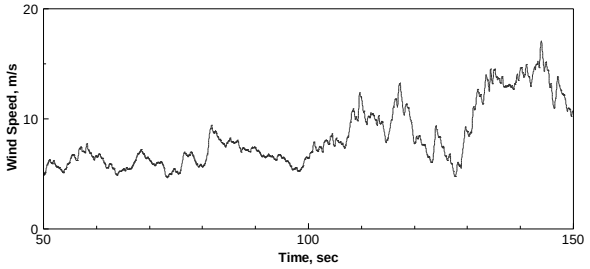

Fig. 1a. Wind Speed Variation

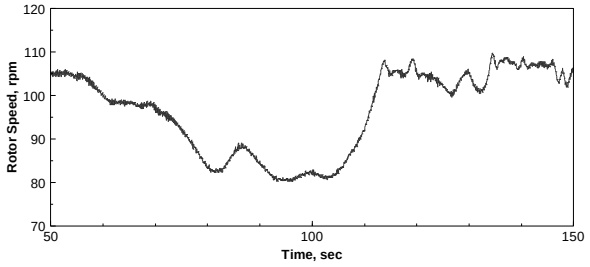

Fig. 1b. RPM Variation

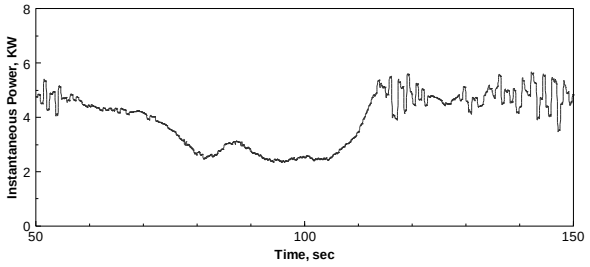

Fig. 1c. Power Production

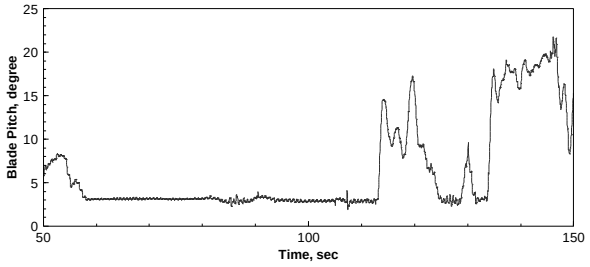

Fig. 1d. Blade Pitch

Fig. 1. Typical Turbine Operation

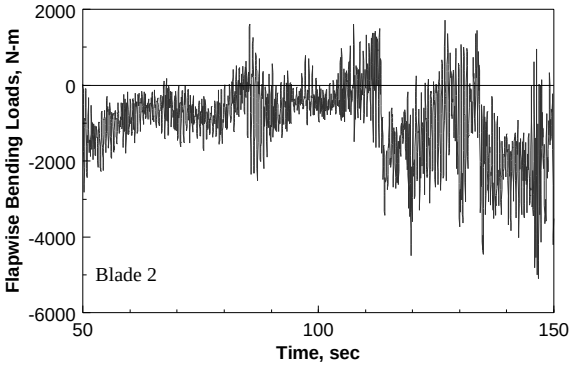

Fig. 2a. Flapwise Bending

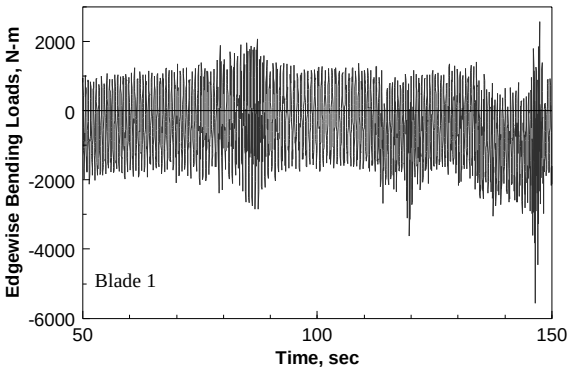

Fig. 2b. Edgewise Bending

Fig. 2. Typical Blade Bending Load Histories

Regions 2 and 3 can be noted by following the variation in the pitch angle of the blade, shown Fig. 1d. In this illustration, the controller switches from Region 3 to Region 2 (i.e., from variable pitch to constant pitch) at approximately 60 seconds, back to Region 3 (i.e., from constant pitch to variable pitch) at approximately 115 seconds. The speed of the turbine starts at approximately 105 rpm, decreases to a low of approximately 80 rpm at approximately 95 seconds and then returns to the set point of 105 rpm, see Fig. 1b. In Region 3, the rotor speed varies from approximately 100 to 109 rpm about this set point. The instantaneous power production is reported in Fig. 1c, with a minimum power production of approximately 2.4 kW near a time of 100 seconds and a maximum of 5.6 kW near the end of this time segment.

Root Bending Loads

Each of the three blades was instrumented with strain gauges to measure the root bending stresses in the flapwise and the edgewise directions; see the study of these loads conducted by Hansen and Laino.[10] Typical bending load histograms are shown in Fig. 2.

Damage Analysis

The damage analysis was performed using the LIFE2 code,[7] a fatigue/fracture mechanics code that is specialized to the analysis of wind turbine components. It is a PC-based, menu-driven code that leads the user through the input definitions required to predict the service lifetime of a turbine component. In the current formulation, the service lifetime of turbine components

may be predicted using either Miner's rule or a linear-elastic crack propagation rule. Only Miner's rule is used here.

The LIFE2 code requires four sets of inputs: 1) the wind-speed distribution for the turbine site as an average annual distribution, 2) the material fatigue properties required by the damage rule being used to predict the service lifetime of the component, 3) a joint distribution of mean stress and stress amplitude (stress states) for the various operational states of the turbine, and 4) the operational parameters for the turbine and the stress concentration factor(s) for the turbine component. The third set of input variables are "cycle-count matrices" that define the load spectrum imposed upon the turbine.

For the calculations presented here, the full capabilities of the LIFE2 code are not required. In particular, we will be comparing the damage contained in constant-speed and variable-speed bins about an approximately constant mean wind speed, rather than predicting service lifetimes. Thus, the wind-speed distribution and most of the operational parameters are not important here and these parts of the analysis procedure are not included in the results cited here. The remaining properties were input into the code as follows.

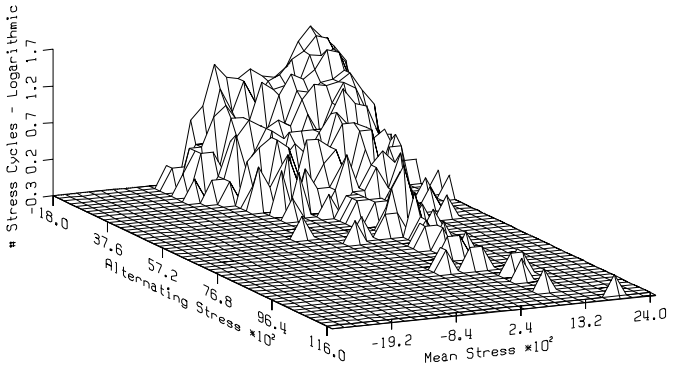

Fig. 3a. Flapwise Cycle Count Distribution

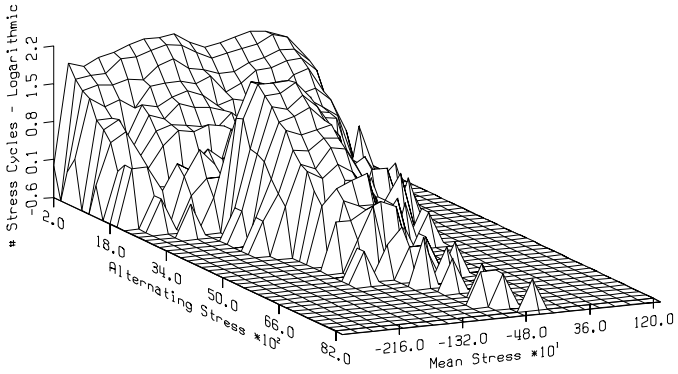

Fig. 3b. Edgewise Cycle Count Distribution

Fig. 3. Cycles Count Matrix for Variable-Speed Operation at Approximately 9 m/s Inflow Velocity

The Blade Root

Following Hansen and Laino[10] and Sutherland and Kelley,[11] we have selected the cylindrical root shank of the rotor as the demonstration location for the damage calculations. This steel root is not typical of the root connection that is currently being used in utility grade wind turbines. Its highly conservative design yields an essentially infinite service lifetime. For the purposes of this demonstration, we will artificially modify this root to reflect a conventional design philosophy. First, we will assume that the root is constructed from a variety of different materials, and second we will change the load/strain conversion so as to bring the damage predictions into a range of interest. The implications of the former are discussed below.

Fatigue Loads

The fatigue load cycles for each of the test cases were determined by rainflow counting[7] 10-minute histograms that were measured during normal operation of the turbine. The histories for all three blades were included in each of the analyses. Typical 3-dimensional plots of the cycle-count matrices for variable-speed operation are shown in Fig. 3. These data and data from an equivalent constant-speed test are summarized in the 2-dimensional plots shown in Figs. 4 and 5. Figure 4 presents the distributions of cycle counts for the alternating stress cycles and Fig. 5 presents the complementary cumulative density function (CDF) for these distributions.

Material Properties

For this example, the blade root is assumed to be constructed from one of three generic materials or a commercial-grade fiberglass composite. For the former, the materials are assumed to have a log-log SN curve of the form:

$$\log(S) = C_1 - \frac{1}{b_1}\log(N) \quad , \qquad [1]$$

where N is the number of cycles to failure at stress level S. Both b and C are material constants. C is

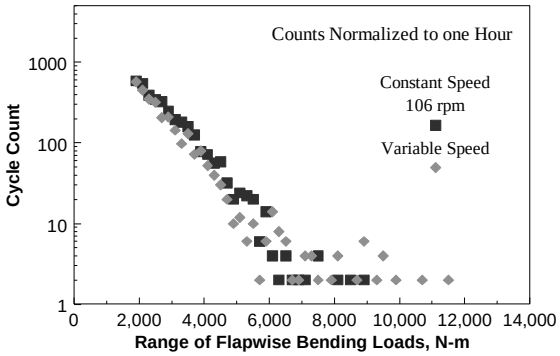

Fig. 4a. Flapwise Cycle Count Distribution

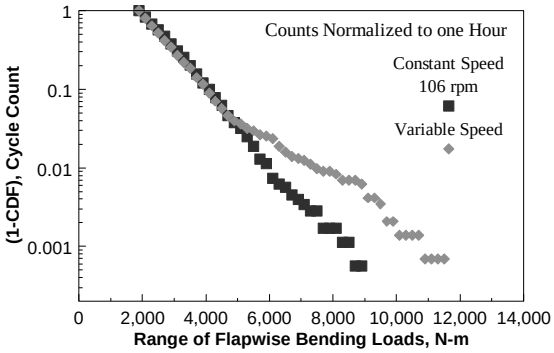

Fig. 5a. Flapwise Cycle Count Distribution

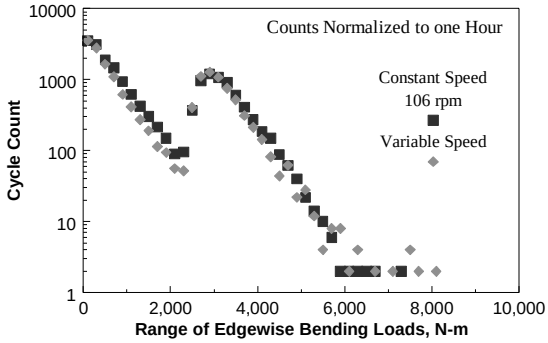

Fig. 4b. Edgewise Cycle Count Distribution

Fig. 4. Alternating Cycles Counts for Constant and Variable-Speed Operation at Approximately 9 m/s Inflow Velocity

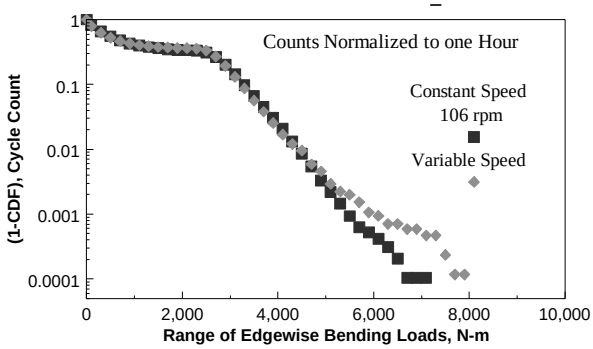

Fig. 5b. Edgewise Cycle Count Distribution

Fig. 5. Complementary Cumulative Density Functions for the Alternating Cycles Counts for Constant and Variable-Speed Operation at Approximately 9 m/s Inflow Velocity

related to the ultimate stress of the material. The constant b is called the fatigue exponent. Three generic materials are used in this analysis, with fatigue exponents of 3, 6 and 9. A fatigue exponent of 3 is typical of welded steel, 6 is typical of aluminum and 9 is typical of composite materials. The dependence of this SN formulation on mean stress is evaluated using Goodman's rule.[7] This formulation yields a symmetric Goodman diagram, i.e., the materials have the same properties in tension and compression.

The final material used in this analysis is the fatigue characterization that has been developed by Mandell and Sutherland[12] for commercial grades of fiberglass composites that are typically used in wind turbines, see Fig. 6. This formulation is based on a log-linear fit of the SN data of the form:

$$S = C_2 - \frac{1}{b_2} \log(N) \quad . \qquad [2]$$

As shown in this figure, this formulation has a highly non-symmetric Goodman diagram.

RESULTS AND DISCUSSION

The Test Cases

The experimental records used here are summarized in Table I. Each record is 10-minutes in length, and the bending loads on all three blades were measured.

In the first case, the control algorithm was set to mimic an induction generator, for constant speed operation. For variable speed, the control algorithm cited above was used. The average wind speed was 5.7 m/s for the constant-speed data set and 5.9 m/s for variable-speed data set. Thus, the inflow conditions are primarily in Region 2 of the variable-speed control algorithm, and case 1 provides the best comparison of

Table I. The Test Cases and Summary of Results

Case Number	Average Wind Speed, m/s		Rotational Speed, rpm				Percent Increase from Constant to Variable Speed	
	Constant	Variable	Constant		Variable		Measured Energy Gain	Efficiency
			Avg	Std Dev	Avg	Std Dev		
1	5.7	5.9	71	1.0	84	11	11	5
2	10.2	9.3	106	1.5	100	9.5	-4	12

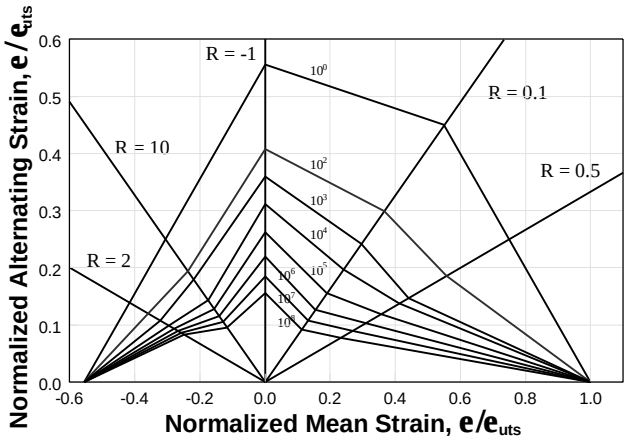

Figure 6. Normalized Goodman Diagram for Fiberglass Composites.

variable-speed operation to constant-speed operation with an induction generator. For the second case, the variable-speed algorithm was used for the variable-speed and the constant-speed data sets. With average wind speeds of 9.3 m/s and 10.2 m/s, respectively, the variable-speed inflow conditions are in both Regions 2 and 3 of the control algorithm and the constant-speed inflow conditions are primarily in Region 3. Thus, case 2 provides a comparison of constant-speed operation under pitch control to operation with transitions between constant-speed operation (Region 2) and variable-speed operation (Region 3).

In both cases, the constant-speed control was able to hold the speed constant within a standard deviation of 1.5 rpm. In the variable-speed and constant torque modes, the turbine speed varied with standard deviations of at least 9.5 rpm.

Energy Comparisons

The measured energy productions for the two cases are compared in Table I. For this comparison, the energy produced by the turbine during the 10-minute record of variable-speed operation is ratioed to that produced during constant-speed operation. The increase in the measured energy production (in percent) is listed in Table I as the measured energy gain. As wind speed is varying during the 10-minute collection period, the energy production is probably not the appropriate measure for comparing constant-speed and variable-speed operation, especially in light of the fact that available energy in the inflow is proportional to the cube of the velocity.

Another, and more enlightening comparison, is the efficiency of power production. This efficiency may be examined by comparing the ratio of the actual power produced by the turbine to the maximum power that can be theoretically produced, i.e., the Betz limit.[13] Namely, the Betz-limit power coefficient, $(C_p)_B$, is given by

$$\left(C_p\right)_B = \frac{\text{Power Produced}}{\left(16/27\right)\left(\frac{1}{2}\, r_o\, U_\infty^3\, A_D\right)} \quad , \qquad [3]$$

where r_o is the air density, U_∞ is the inflow velocity, and A_D is the swept area of the rotor.

The average Betz-limit power coefficient was computed for the case studies using the instantaneous power production and the corresponding inflow velocity. The comparison of these coefficients is reported in Table I as the efficiency. In case 1, the efficiency of power conversion for variable-speed operation is 5 percent greater than the constant-speed efficiency. In case 2, variable speed is 12 percent greater than constant speed.

Load Comparison

As shown in Fig. 4, the body of the cyclic load distributions from variable-speed and constant high-speed operation are very similar to one another. However, there is a significant difference in the high-stress low-cycle tail of the distribution. In particular, the variable-speed algorithm is introducing a comparatively large number of high-stress cycles into the load spectrum.

In their simulations of variable-speed operation, both Moroz, Swift and VandenBosche[4] and Quarton and Wei[5] note that variable-speed operation increases blade loads. Moreover, the former simulation not only predicts increased blade loads, but it also predicts increased tower loads.

Damage Comparisons

Of particular importance in damage analysis is the material properties used in that analysis. As discussed by Winterstein and Lange,[14] material properties play a significant role in determining which portion of the load spectrum dominates predictions of service lifetimes. With a relatively low fatigue exponent, the body of the distribution will dominate, and with a relatively high fatigue exponent, the high-stress, low-cycle tail of the distribution will dominate. The damage results reported in Table II for the generic materials with fatigue exponents of 3, 6 and 9 illustrate this trend, with the high-stress tail having little effect on damage with a fatigue exponent of 3 (for both cases, the predicted service lifetime is reduced by a maximum factor of 2.7) and a significantly higher effect with a fatigue exponent of 9 (a factor of 7.7). Thus, the high fatigue-exponent analysis emphasizes the importance of the load cycles that have been added to the tail of the distribution by variable-speed operation.

The addition of the high-stress cycles into the load spectrum under variable-speed operation are even more significant when measured using the fatigue characterization for commercial grades of fiberglass composites, see Table II. In case 1, the damage rate is increased by a factor greater than 70 and in case 2, it is increased by a factor greater than 40.

Discussion

Thus, the variable-speed control algorithm increases the efficiency of energy production while producing a very large increase in damage (significant decrease in service lifetime) for blade materials with high fatigue exponents. And, for the turbine and the control algorithm used in this study, variable-speed operation is probably not economically advantageous over constant-speed operation.

To determine if the inclusion of variable speed in the design of the turbine is cost effective a complete cost analysis, based on anticipated failure rates,[15] must be conducted. The trade-off analysis can be conducted from the reduced service lifetime prospective discussed above or from a structural load perspective. For the latter, the blade and other structural components may have to be strengthened (with the associated increase in capital costs) to maintain service lifetime under the additional fatigue loads imposed upon the structure by variable-speed operation.

CONCLUDING REMARKS

Variable speed offers the promise of increased energy production and reduced loads through torque control. However, as illustrated in this case history, the promise is not necessarily fulfilled. In this particular study, variable speed adds little or no power production and significantly increases the damage. As the control system used here is rather primitive, with its discrete controls and limited switching options, these results should not be generalized to other control systems. Rather, they illustrate that the inclusion of damage analysis in the evaluation of a variable-speed control system is required to obtain the entire picture of its benefits and consequences.

REFERENCES

1. L.J. Fingersh and M.C. Robinson, "The Effects of Variable Speed and Drive Train Component Efficiencies on Wind Turbine Energy Capture," *1997 ASME Wind Energy Symposium*, W. Musial, ed., ASME, 1997.

2. E. Muljadi, C.P. Butterfield and M.L. Buhl, Jr., "Effects of Turbulence on Power Generation for Variable-Speed Wind Turbines," *1997 ASME Wind Energy Symposium*, W. Musial, ed., ASME, 1997.

3. A.D. Wright, M.L. Buhl, Jr. And G.S. Bir, "An Examination of Loads and Responses of a Wind Turbine Undergoing Variable-Speed Operation," *1997 ASME Wind Energy Symposium*, W. Musial, ed., ASME, 1997.

4. E.M. Moroz, A.H.P. Swift and J.H. VandenBosche, "Evaluating Fatigue Loades Under Variable Speed Operation," *Wind Energy 1998*, ASME/AIAA, in publication.

5. D.C. Quarton and J. Wei, "The Strucural Implications of Variable Speed Operation," *EWEC '91*, Elsevier, 1991.

6. P.W. Carlin and L.J. Fingersh, "Some Preliminary Results from the NWTC Direct-Drive, Variable-Speed Test Bed," *1997 ASME Wind Energy Symposium*, W. Musial, ed., ASME, 1997.

7. H.J. Sutherland and L.L. Schluter, "The LIFE2 Computer Code, Numerical Formulation and Input Parameters," *Proceedings of WindPower '89*, SERI/TP-257-3628, 1989.

8. C.P. Butterfield, W.P. Musial, G.N. Scott, D.A. Simms, *NREL Combined Experiment Final Report—Phase II*, NREL/TP-442-4807, National Renewable Energy Laboratory, Golden, Colorado, 1992.

9. E.F. Fuchs, A.A. Fardoun, P.W. Carlin, and R.W. Erickson, "Permanent-Magnet Machines for Operation with Large Speed Variations," *Proceedings of WindPower '92* , AWEA, 1992.

10. A.C. Hansen and D.J. Laino, "Validation Study for AeroDyn and YawDyn Using Phase III Combined Experiment Data," *1997 ASME Wind Energy Symposium*, W. Musial, ed., ASME, 1997.

11. H.J. Sutherland and N.D. Kelley, "Fatigue Damage Estimate Comparisons for Northern European and U.S. Wind Farm Loading Environments," *Proceedings of WindPower '95*, AWEA, 1995.

12. H.J. Sutherland and J.F. Mandell, "Application of the U.S. High Cycle Fatigue Data Base to Wind Turbine Blade Lifetime Predictions," *Energy Week 1996, Book VIII: Wind Energy*, Musial and Berg, eds., ASME, 1996.

13. L.L. Freris, *Wind Energy Conversion Systems*, Prentice Hall, 1989.

14. S.R. Winterstein and C.H. Lange, "Load Models for Fatigue Reliability from Limited Data," *Wind Energy 1995*, Musial, Hock and Berg, eds., SED-Vol. 16 ASME, 1995.

15. P.S. Veers, "Fatigue Reliability of Wind Turbine Fleets: The Effect of Uncertainty on Projected Costs," *Wind Energy 1996*, Vol. 1, Energy Week, ASME, 1996.